



LUND UNIVERSITY

Experimental and theoretical studies of lifetimes and transition probabilities for Au II

Zhiguo, Zhang; Brage, Tomas; Curtis, LJ; Lundberg, Hans; Martinson, Indrek

Published in:

Journal of Physics B: Atomic, Molecular and Optical Physics

DOI:

[10.1088/0953-4075/35/3/303](https://doi.org/10.1088/0953-4075/35/3/303)

2002

[Link to publication](#)

Citation for published version (APA):

Zhiguo, Z., Brage, T., Curtis, L.J., Lundberg, H., & Martinson, I. (2002). Experimental and theoretical studies of lifetimes and transition probabilities for Au II. *Journal of Physics B: Atomic, Molecular and Optical Physics*, 35(3), 483-490. <https://doi.org/10.1088/0953-4075/35/3/303>

Total number of authors:

5

General rights

Unless other specific re-use rights are stated the following general rights apply:

Copyright and moral rights for the publications made accessible in the public portal are retained by the authors and/or other copyright owners and it is a condition of accessing publications that users recognise and abide by the legal requirements associated with these rights.

- Users may download and print one copy of any publication from the public portal for the purpose of private study or research.
- You may not further distribute the material or use it for any profit-making activity or commercial gain
- You may freely distribute the URL identifying the publication in the public portal

Read more about Creative commons licenses: <https://creativecommons.org/licenses/>

Take down policy

If you believe that this document breaches copyright please contact us providing details, and we will remove access to the work immediately and investigate your claim.

LUND UNIVERSITY

PO Box 117
221 00 Lund
+46 46-222 00 00

Experimental and theoretical studies of lifetimes and transition probabilities for Au II

This article has been downloaded from IOPscience. Please scroll down to see the full text article.

2002 J. Phys. B: At. Mol. Opt. Phys. 35 483

(<http://iopscience.iop.org/0953-4075/35/3/303>)

View [the table of contents for this issue](#), or go to the [journal homepage](#) for more

Download details:

IP Address: 130.235.188.104

The article was downloaded on 05/07/2011 at 08:51

Please note that [terms and conditions apply](#).

Experimental and theoretical studies of lifetimes and transition probabilities for Au II

Zhang Zhiguo¹, T Brage², L J Curtis³, H Lundberg¹ and I Martinson²

¹ Department of Physics, Lund Institute of Technology, Box 118, SE-221 00 Lund, Sweden

² Department of Physics, Lund University, Box 118, SE-221 00 Lund, Sweden

³ Department of Physics and Astronomy, University of Toledo, Toledo, OH 43606, USA

Received 15 June 2001, in final form 30 October 2001

Published 24 January 2002

Online at stacks.iop.org/JPhysB/35/483

Abstract

We report lifetime measurements for three of the $5d^96p$ levels in Au II and relativistic multiconfiguration Dirac–Fock (MCDF) calculations of lifetimes and transitions probabilities in this ion. The work was motivated by significant disagreements between previous experimental $5d^96p$ lifetimes, obtained by means of the beam–foil (BF) method and theoretical data based on Hartree–Fock calculations in which relativistic effects were included as perturbations. The new measurements, based on laser-induced fluorescence, support the BF data and are also in excellent agreement with the MCDF results. We confirm that, while computational methods which include perturbative relativistic corrections appear to be adequate for moderately heavy elements such as Ag, fully relativistic calculations are essential for describing systems as heavy as Au.

1. Introduction

Much interest has been focused in recent years on the structure and spectra of neutral, singly and doubly ionized heavy atoms. Theoretical and experimental studies of such species are often motivated by recent progress in stellar spectroscopy with the Hubble Space Telescope (HST), particularly of the chemically peculiar (CP) stars which have very high abundances of heavy elements. For instance, in the star χ Lupi the elements Ru and Pd are overabundant by two orders of magnitude and Pt, Au and Hg are overabundant by 4–5 orders of magnitude, in comparison with their solar abundances, see Wahlgren *et al* (1995) and Brandt *et al* (1999). A wealth of atomic data, including wavelengths, transition probabilities, radiative lifetimes, hyperfine structure separations and isotope shifts are required for successful analyses of such stellar spectra (Leckrone *et al* 1993).

In this paper we report new experimental and theoretical data for lifetimes and transition probabilities for singly ionized gold, Au II. While these quantities have been studied earlier, there exist significant discrepancies between the experimental and theoretical values. This circumstance has largely motivated the present investigation.

2. Survey of previous work

The spectrum and energy levels of Au II were thoroughly studied some years ago (Rosberg and Wyart 1997) by means of high-resolution emission spectroscopy and theoretical calculations using the program package of Cowan (1981). The results include about 450 classified spectral lines and 120 energy levels. The ground term $5d^{10}$ and the excited configurations $5d^96s$, $5d^96p$, $5d^96d$ and $5d^97s$ are now completely known, whereas only one level (1S) is missing for the $5d^86s^2$ configuration. For astrophysics the transitions from $5d^96p$ (12 levels) to $5d^96s$ (4 levels) are of particular interest. Of these lines the $6s(5/2, 1/2)_3-6p(5/2, 3/2)_4$ combination, at 1740.476 \AA , $6s \ ^3D_3-6p \ ^3F_4$ in LS notation, has been observed in χ Lupi and used for the determination of the gold abundance in this star (Wahlgren *et al* 1995).

Lifetimes of 11 of the $5d^96p$ levels were determined some years ago by Beideck *et al* (1993a) who used the beam-foil (BF) excitation technique. The experimental values ranged from 1.4–3.8 ns, while the uncertainties were estimated to lie in the interval 12–20%. The main problems when using this technique are caused by cascading, i.e. feeding of the level under study from higher-lying levels, and by line blends. In the Au II case cascading is expected from various $5d^97s$ and $5d^96d$ levels whereas blends mainly arise from Au III transitions. This particular spectrum has been analysed by Iglesias (1966). However, Beideck *et al* could conclude that these problems were not too disturbing. Thus, the Au II $6p-6d$ and $6p-7s$ cascade transitions were quite weak in the BF spectra. With a few exceptions, one of which will be discussed below, the same could be noted for the Au III lines.

Furthermore, Beideck *et al* (1993a) also reported theoretical lifetime values for all the $6p$ levels, calculated with the Cowan code in the relativistic Hartree-Fock mode. However, these theoretical lifetimes were typically about 30% shorter than the experimental ones, and thus well outside the experimental uncertainties. In view of this difference a new calculation was performed (Bogdanovich and Martinson 2000). Here an elaborate superposition of configurations (SOC) code, developed by Bogdanovich, was applied. However, the resulting lifetimes and transition probabilities were in very good agreement with the previous theoretical results (Beideck *et al* 1993a) as well as with the subsequent Cowan-code calculations (Rosberg and Wyart 1997).

To further explore the origin of this discrepancy between theory and experiment we have now made novel measurements using the method of laser-induced fluorescence (LIF) as well as new calculations with the relativistic multiconfiguration Dirac-Fock (MCDF) code.

3. Laser experiments

Lifetimes for three of the Au II $5d^96p$ levels were remeasured using the LIF method. Compared to the BF technique LIF provides selective excitation of the studied levels and the observed fluorescence is thus free from cascades. The method, however, does not have the broad applicability of the BF technique in the excitation-energy range and in the vacuum-ultraviolet (VUV) spectral region. The three remeasured energy levels were chosen due to their strong excitation and decay channels to fairly low metastable levels at ultraviolet wavelengths.

In the experiments Au ions were created in a plasma produced by focusing a pulsed laser beam onto a gold target. The laser pulses had a duration of 15 ns and energy of about 50 mJ. A typical velocity for a singly ionized Au ion was then $5 \times 10^3 \text{ m s}^{-1}$. The measurements were performed close to the target during the plasma expansion. (For a diagram of the experimental set-up, see, e.g., Li *et al* (2000).) In the plasma, metastable levels belonging to the $5d^96s$ configuration were populated and used as a starting point for laser excitation to the $5d^96p$ levels under investigation. Pulsed tunable laser radiation was produced by a Nd:YAG laser system.

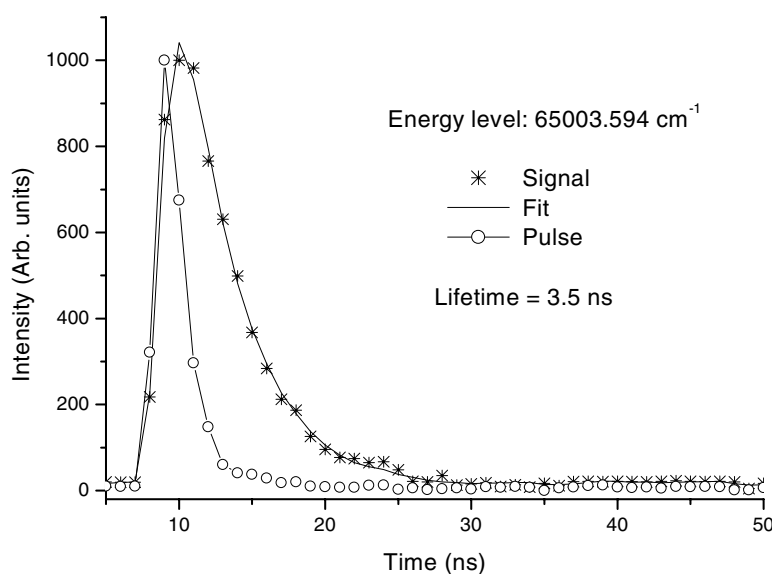


Figure 1. Recordings of the excitation pulse and subsequent fluorescence signal for the $65\,003.594\text{ cm}^{-1}$ level. A convolution procedure gives the lifetime as 3.5 ns.

Conventional Nd:YAG lasers provide pulses with a duration of about 10 ns, but for precision lifetime measurements the excitation pulse must be shorter than the investigated lifetime. The pulses were therefore compressed to 1 ns utilizing stimulated Brillouin scattering in a water cell (Schiemann *et al* 1997) and thereafter pumped a tunable dye laser working on a red dye. The dye laser light was then converted to wavelengths around 2100 \AA using frequency tripling in non-linear crystals. The conversion efficiency in these crystals is about 10%. Laser spectroscopy in the VUV is mainly hampered by the lack of VUV transparent crystals. In this region conversion has to be performed in gases with much lower efficiency. In our measurements the energy of the 2100 \AA pulses was about 1 mJ.

Fluorescent light released at the decay of the excited levels was detected using a monochromator and a fast photomultiplier in a direction perpendicular to both the excitation beam and the flight direction of the ions. The data acquisition was performed by a digital transient recorder with a 1 GHz bandwidth and a 2 GS s^{-1} sampling rate. The temporal shape of the excitation pulse was recorded with the same detection system by detecting the scattered light of the laser pulse from a metal rod, which was inserted into the interaction point of the Au ions and the excitation beam. The recorded pulse is the convolution of the real laser pulse and the time response function of the detection system. By fitting the fluorescence signal to the convolution of the detected laser pulse and a pure exponential function, the effects of the finite duration of the excitation laser pulse and the limited response time of the detection system are taken into account. To ensure the precision of this convolution fitting, neutral-density filters were inserted in the excitation laser beam to reduce the power, which effectively prevented saturation of the excitation. A decay curve and the corresponding convolution fit are shown in figure 1.

The bandwidth of the laser light utilized in the investigations was about 0.1 \AA . After setting the laser to the excitation wavelength (taken from Rosberg and Wyart (1997)), a further test of proper level identification was made in our measurements. All the possible decay channels (1–4 such channels for each $5d^96p$ level) were checked by tuning the monochromator.

Table 1. Lifetimes of the $5d^96p$ levels in Au II.

Term	J	Energy ^a (cm^{-1})	$\lambda^{a,b}$ (\AA)	Lifetime (ns)			
				Experiment ^c		Theory ^d	
(5/2, 1/2)	3	65 003.594	2110.68	3.5(3)	3.5(5)	3.45	1.99
(5/2, 1/2)	2	63 053.318	2082.07	3.8(3)	3.8(5)	3.65	2.04
(5/2, 3/2)	4	72 495.129	1740.48		2.4(3)	2.03	1.48
(5/2, 3/2)	3	74 791.477	1673.59		2.4(4)	1.98	1.41
(5/2, 3/2)	2	73 178.291	1800.58		2.6(5)	2.31	1.59
(5/2, 3/2)	1	73 403.839	1793.30		2.3(4)	2.42	1.16
(3/2, 1/2)	2	76 659.700	2044.59	3.4(5)	2.5(4)	3.28	1.96
(3/2, 1/2)	1	81 659.828	1224.59		1.4(3)		0.72
(3/2, 3/2)	3	85 700.201	1783.20		2.5(4)	2.09	1.55
(3/2, 3/2)	2	86 565.667	1700.68		2.4(4)	2.11	1.44
(3/2, 3/2)	1	85 707.570	1725.87		1.8(3)	2.05	0.94
(3/2, 3/2)	0	82 613.781	1823.22			2.34	1.69

^a Rosberg and Wyart (1997).

^b The most intense line from this level. The wavelengths have been rounded off.

^c Present work, first column; Beideck *et al* (1993a), second column.

^d Present work, first column; Bogdanovich and Martinson (2000), dipole length values, second column.

To ensure a linear response of the detection system, only sufficiently weak fluorescence signals, subsequent to each excitation pulse, were sampled. An average of 1000–4000 pulses was necessary for each curve, depending on the signal-to-noise ratio.

The new lifetime data from the LIF investigations are presented in table 1. The quoted error bars of the reported lifetimes represent conservative estimates of the combined random and systematic errors. The standard deviations of different measurements are less than 50% of the quoted uncertainties. For the $76\,659.700\text{ cm}^{-1}$ level laser excitation was performed from a rather high $6s$ metastable level. Increasing the energy of the laser pulses creating the plasma to 100 mJ, and thus also increasing the density and temperature of the Au plasma, generated sufficient population of this metastable level. This also increased the risk for systematic errors such as collisional quenching and flight-out-of-view effects. The lifetime for this level is therefore given with larger error bars.

4. Theoretical calculations

During the last few years a systematic approach has been developed for heavy atomic systems, including a careful treatment of valence as well as core–valence correlation (see, for example, Brage *et al* (1996, 1999a, 1999b)). These calculations have been motivated by a large need for atomic parameters for these systems (e.g. Wahlgren *et al* (1995) and Proffitt *et al* (1999)). The method used is a fully relativistic MCDF approach, utilizing the GRASP94 code (Parpia *et al* 1996) with extensive inclusion of configuration interaction. A similar method was also applied to the Hg III system, which is isoelectronic to Au II (Beideck *et al* 1993b, Henderson *et al* 1999).

The details of the MCDF are described in a number of earlier papers (see Brage *et al* (1999b) and references therein) and we will here only emphasize some of the most important properties for our discussion. The atomic system is represented by a J -dependent atomic state

function, which is a linear combination of configuration state functions (CSFs):

$$\Psi(\gamma J) = \sum_k c_k \Phi(\alpha_k J). \quad (1)$$

The CSFs are created as coupled, antisymmetric products of spin-orbitals, where the spin-angular parts are known, while the radial parts are determined from solving the integro-differential equations of the MCDF procedure. To define a suitable functional, from which the energy expression is defined and the MCDF equations are derived, we use a weighted average of a set of energies. We will use two different procedures. The extended average level (EAL) method implies that all possible eigenvalues are included in the functional. In the extended optimal level (EOL) approach we only select a subset of eigenvalues. Various approaches and problems with the self-consistent inclusion of the Breit interaction have been discussed by Kim *et al* (1998).

In earlier papers we have used a number of different approaches to generate CSFs, defining the functional and optimizing the radial functions. In this study we will use the active set, cross-optimization technique (Brage *et al* (1999b) and references therein). According to this we will define an active set of orbitals, together with some constraints, from which we generate CSFs. The radial functions are optimized in steps, using different sets of eigenvalues to generate an MCDF functional. This gives us an efficient approach to represent all the levels of interest.

The ground configuration of Au II is of the form $5d^{10}$, while the two excited configurations of interest here are $5d^9 6s$ and $5d^9 6p$ (we omit all closed subshells inside the $5d$). Our first step is to optimize all the closed subshell orbitals, together with the $5d$, $6s$ and $6p$ on an EAL calculation, including all the CSFs belonging to these two configurations. As a second step, we include correlation between the ' $5d^9$ ' core and the outer $n = 6$ electron by including all CSFs with at least eight $5d$ electrons and a new set of orbitals with the symmetry s , p , d and f in the active set. These new orbitals are optimized on the lowest 12 odd states, belonging to the $5d^9 6p$ configuration. Yet another set of orbitals, with symmetry s , p and d , are then optimized on the four states with main components of the $5d^9 6s$ configuration. The total orbitals in the active set are now three s - and p -orbitals, two d -orbitals and one f -orbital. These are used in a final configuration interaction calculation, including all odd CSFs with $J \in \{0, 1, 2, 3, 4\}$ and even CSFs with $J \in \{2, 3, 4\}$. From this model we compute gf values and transition probabilities that are reported in tables 1–3.

Table 1 includes present and previous experimental and computed lifetimes, whereas table 2, which gives the experimental and theoretical energy levels, shows that our new calculations represent the two configurations ($5d^9 6s$ and $5d^9 6p$) in a balanced way. Table 3 provides the experimental wavelengths and recommended gf values for all transitions between the two configurations. The recommended gf values are computed from theoretical line strengths and experimental wavelengths. (We here use LS notation for the lower levels and jj notation for the higher ones.)

5. Discussion

A study of table 1 makes it clear that agreement between the new experiments, performed with the LIF technique and the relativistic MCDF calculations, is quite satisfactory. There is also good accord between the BF data and the new results. The only exception can be noted for the $76\,659.700\text{ cm}^{-1}$ level, mentioned above. Here the LIF and MCDF lifetimes are significantly longer than the BF result. Beideck *et al* (1993a) suspected a blend from an Au III transition here, and it now appears that this is indeed the case.

A similar agreement between BF data and MCDF results was recently established for the lifetimes of $5d^9 6p$ levels in Hg III (see Henderson *et al* (1999)). We may therefore conclude

Table 2. Experimental (from Rosberg and Wyart (1997)) and theoretical energies relative to the lowest 6s level, 6s ³D₃.

Level designation	<i>J</i>	<i>E</i> _{exp}	<i>E</i> _{th}
6s ³ D	3	0.0	0.0
6s ³ D	2	2 601.044	2 635.3
6s ³ D	1	12 726.186	12 334.7
6s ¹ D	2	14 581.677	14 306.5
6p(5/2, 1/2)	2	48 013.746	47 748.3
6p(5/2, 1/2)	3	49 964.022	49 830.8
6p(5/2, 3/2)	4	57 455.557	57 031.8
6p(3/2, 1/2)	1	58 364.267	57 983.2
6p(5/2, 3/2)	2	58 138.719	58 124.7
6p(5/2, 3/2)	3	59 751.905	60 015.7
6p(3/2, 1/2)	2	61 620.128	61 321.5
6p(5/2, 3/2)	1	66 620.256	66 423.4
6p(3/2, 3/2)	0	67 574.209	66 732.9
6p(3/2, 3/2)	3	70 660.629	70 092.2
6p(3/2, 3/2)	1	70 667.998	70 369.3
6p(3/2, 3/2)	2	71 526.095	71 525.8

that theoretical calculations, which treat the relativistic effects as perturbations, are not entirely satisfactory for heavy systems such as Au and Hg. Fully relativistic calculations of the MCDF type, for instance, must be applied in such cases. It is interesting to compare the present results with similar data for Ag II, which is homologous to Au II. The ground term is now 4d¹⁰ ¹S and the lowest excited configurations are 4d⁹5s, 4d⁸5s² and 4d⁹5p. Using the BF method Irving *et al* (1995) determined the lifetimes of all 5p levels. As in the Au II case these experimental values were significantly longer than theoretical data, based on the Cowan-type calculations or those performed using the Coulomb approximation Hartree–Slater (CAHS) method. Somewhat later a beam–laser (BL) study of Ag II lifetimes was reported (Biemont *et al* 1997) but here the results for the 5p levels were approximately 20% shorter than the BF results of Irving *et al* (1995). The BL method is superior to the BF one, although not as general. Thus, cascading and line blending are avoided because of the state-selective excitation. Furthermore, the BL data were in good agreement with theoretical values included in these two—preferentially experimental—Ag II papers and also with later results of elaborate *ab initio* calculations (Bogdanovich and Martinson 1999). We can therefore conclude that the experimental uncertainties may have been too optimistic in the BF study of Ag II.

It is interesting to note that there are semiclassical analogues to this switch-on of relativistic effects between Ag and Au. This was noticed in a semiclassical self-consistent-field calculation (Curtis and Silbar 1984) that was made for the isoelectronic sequence of the homologous atom Cu. This calculation used the position probability densities of electrons in their various classical orbits, as specified by the Einstein–Brillouin–Keller (EBK) semiclassical quantization condition, to compute a self-consistent charge distribution. This approach yielded nonrelativistic results for the energies of the individual orbitals that agreed very closely with standard Hartree–Fock calculations. However, when the calculations were generalized by use of the relativistic momentum, two abrupt discontinuities as a function of *Z* appeared in the core charge distribution. Both occurred in the vicinity of *Z* = 60, approximately midway between *Z* = 47 and 79, the nuclear charges of Ag and Au.

The first discontinuity concerned the relative positions of the outer turning points (apiapses) of the 1s orbits and the inner turning points (periapses) of the *np* orbits, which have a *Z*-dependent differential screening. For *Z* ≪ 60, the *np* periapses were inside the 1s apiapses, whereas for *Z* ≫ 60 the *np* periapses were outside the 1s apiapses. Moreover, the transition

Table 3. Experimental wavelengths (from Rosberg and Wyart 1997) and recommended gf values (from theoretical line strengths and experimental transition energies) for 6s–6p transitions in Au II.

λ_{exp} (Å)	Lower	Upper	gf_{rec}
2990.2681	6s 1D_2	6p(5/2, 1/2) ₂	1.03E–2
2833.86 ^a	6s 3D_1	6p(5/2, 1/2) ₂	1.41E–3
2825.4370	6s 1D_2	6p(5/2, 1/2) ₃	1.10E–2
2295.84 ^a	6s 1D_2	6p(5/2, 3/2) ₂	1.21E–5
2283.3078	6s 1D_2	6p(3/2, 1/2) ₁	6.29E–2
2213.1571	6s 1D_2	6p(5/2, 3/2) ₃	3.50E–2
2201.3400 ^b	6s 3D_2	6p(5/2, 1/2) ₂	2.46E–2
2201.3400 ^b	6s 3D_1	6p(5/2, 3/2) ₂	5.35E–2
2191.15 ^a	6s 3D_1	6p(3/2, 1/2) ₁	3.65E–3
2125.2486	6s 1D_2	6p(3/2, 1/2) ₂	3.73E–1
2110.6847	6s 3D_2	6p(5/2, 1/2) ₃	8.52E–1
2082.0737	6s 3D_3	6p(5/2, 1/2) ₂	8.63E–1
2044.5869	6s 3D_1	6p(3/2, 1/2) ₂	5.15E–1
2000.7919	6s 3D_3	6p(5/2, 1/2) ₃	4.47E–1
1921.6513	6s 1D_2	6p(5/2, 3/2) ₁	4.52E–1
1855.4924	6s 3D_1	6p(5/2, 3/2) ₁	9.48E–2
1823.22 ^a	6s 3D_1	6p(3/2, 3/2) ₀	2.13E–1
1800.58 ^a	6s 3D_2	6p(5/2, 3/2) ₂	9.75E–1
1783.1995	6s 1D_2	6p(3/2, 3/2) ₃	1.53E 0
1782.9678	6s 1D_2	6p(3/2, 3/2) ₁	1.04E–1
1756.0981	6s 1D_2	6p(3/2, 3/2) ₂	6.27E–1
1749.7563	6s 3D_2	6p(5/2, 3/2) ₃	5.29E–1
1740.4751	6s 3D_3	6p(5/2, 3/2) ₄	2.01E 0
1725.8685	6s 3D_1	6p(3/2, 3/2) ₁	5.05E–1
1720.0239	6s 3D_3	6p(5/2, 3/2) ₂	3.74E–2
1700.6820	6s 3D_1	6p(3/2, 3/2) ₂	4.06E–1
1694.3672	6s 3D_2	6p(3/2, 1/2) ₂	5.70E–2
1673.5869	6s 3D_3	6p(5/2, 3/2) ₃	9.77E–1
1622.8466	6s 3D_3	6p(3/2, 1/2) ₂	7.50E–3
1562.0312	6s 3D_2	6p(5/2, 3/2) ₁	8.66E–2
1469.3008	6s 3D_2	6p(3/2, 3/2) ₃	3.37E–2
1469.1424	6s 3D_2	6p(3/2, 3/2) ₁	3.76E–2
1450.8514	6s 3D_2	6p(3/2, 3/2) ₂	1.40E–2
1415.2149	6s 3D_3	6p(3/2, 3/2) ₃	8.03E–3
1398.0912	6s 3D_3	6p(3/2, 3/2) ₂	9.43E–3

^a Transition not observed by Rosberg and Wyart (1997), wavelength computed from experimental level energies.

^b Two lines coincide and probably observed as one by Rosberg and Wyart (1997).

between these two conditions was very abrupt and exhibited a hysteresis affect, depending on whether the initial values for the self-consistent calculation were taken in increasing or decreasing order of Z . The np periapses remained trapped on one side of the $1s$ apiapses for many stages of ionization past $Z = 60$ before suddenly bursting through, and did so when approached from either side of $Z = 60$.

The second discontinuity concerns the small but finite periapses of the ns orbitals that occur because of the Maslov index ($1/4$ the number of classical turning points) factor in the EBK quantization. In EBK the semiclassical angular momentum is $L = (l + 1/2)\hbar$ rather than $L = \sqrt{l(l + 1)}\hbar$ and is therefore nonzero for $l = 0$. In the relativistic case the expression for the inner classical turning point for an s orbital becomes complex for $Z > 1/2\alpha = 68.5$ causing a singularity that is not present for the nonrelativistic case.

Although these two classical effects provide only an interesting curiosity, such conceptual models often have a quantum mechanical counterpart that may be concealed by the numerical nature of quantum mechanical calculations.

6. Conclusion

We have presented new experimental and theoretical results for lifetimes in Au II. These have removed the previous discrepancy between theory and experiment in this ion. Thus, it is clear that fully relativistic calculations are needed for such a heavy system, whereas basically non-relativistic theories may be sufficient in the case of Ag II. This confirms theoretical comments made earlier by several authors. For example, the importance of relativistic effects on the resonance transitions in neutral Au has been discussed by Desclaux and Kim (1975). We can therefore agree with the statement that ‘the chemical difference between silver and gold may mainly be a relativistic effect’ (Desclaux and Pyykkö 1976).

Acknowledgments

The support from Professor S Svanberg is gratefully acknowledged. We also thank Professors P Bogdanovich and P Pyykkö for enlightening discussions and the referees for valuable remarks. The work has been supported by the Swedish Natural Science Research Council, NFR, and the US Department of Energy.

References

- Beideck D J *et al* 1993a *J. Opt. Soc. Am. B* **10** 977–81
Beideck D J *et al* 1993b *Phys. Rev. A* **47** 884–9
Biemont E, Pinnington E H, Kernahan J A and Rieger G 1997 *J. Phys. B: At. Mol. Opt. Phys.* **30** 2067–73
Bogdanovich P and Martinson I 1999 *Phys. Scr.* **60** 217–20
Bogdanovich P and Martinson I 2000 *Phys. Scr.* **61** 142–5
Brage T, Leckrone D S and Froese Fischer C 1996 *Phys. Rev. A* **53** 192–200
Brage T, Proffitt C and Leckrone D S 1999a *Astrophys. J.* **513** 524–34
Brage T, Proffitt C and Leckrone D S 1999b *J. Phys. B: At. Mol. Opt. Phys.* **32** 3183–92
Brandt J C *et al* 1999 *Astron. J.* **117** 1505–48
Cowan R D 1981 *The Theory of Atomic Structure and Spectra* (Berkeley, CA: University of California Press)
Curtis L J and Silbar R R 1984 *J. Phys. B: At. Mol. Phys.* **17** 4087–101
Desclaux J P and Kim Y-K 1975 *J. Phys. B: At. Mol. Phys.* **8** 1177–82
Desclaux J P and Pyykkö P 1976 *Chem. Phys. Lett.* **39** 300–3
Henderson M, Irving R E, Curtis L J, Martinson I, Brage T and Bengtsson P 1999 *Phys. Rev. A* **59** 4068–70
Iglesias L 1966 *J. Res. NBS A* **70** 465–85
Irving R E *et al* 1995 *Phys. Scr.* **51** 351–3
Kim Y-K, Parente F, Marques J P, Indelicato P and Desclaux J P 1998 *Phys. Rev. A* **58** 1885–8
Leckrone D S, Johansson S, Wahlgren G M and Adelman S J 1993 *Phys. Scr. T* **47** 149–56
Li Z S, Lundberg H, Wahlgren G M and Sikström C M 2000 *Phys. Rev. A* **62** 325 05
Parpia F A, Froese Fischer C and Grant I P 1996 *Comput. Phys. Commun.* **94** 249–71
Proffitt C *et al* 1999 *Astrophys. J.* **512** 942–60
Rosberg M and Wyart J-F 1997 *Phys. Scr.* **55** 690–706
Schiemann S, Ubachs W and Hogervorst W 1997 *IEEE J. Quantum Electron.* **33** 358–66
Wahlgren G M, Leckrone D S, Johansson S G, Rosberg M and Brage T 1995 *Astrophys. J.* **444** 438–51